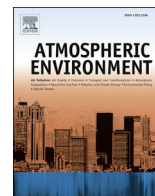




Contents lists available at ScienceDirect

Atmospheric Environment

journal homepage: www.elsevier.com/locate/atmosenv

Effect of heterogeneous aqueous reactions on the secondary formation of inorganic aerosols during haze events



Jiannong Quan^{a, b, *}, Quan Liu^{a, b, **}, Xia Li^a, Yang Gao^a, Xingcan Jia^a, Jiujiang Sheng^{a, b}, Yangang Liu^c

^a Beijing Key Laboratory of Cloud, Precipitation and Atmospheric Water Resources, Beijing, China

^b Institute of Urban Meteorology, Chinese Meteorological Administration, Beijing, China

^c Brookhaven National Laboratory, Upton, NY 11973, USA

H I G H L I G H T S

- Heterogeneous aqueous reactions during haze events was investigated.
- The conversion of gas-phase of S and N to particle-phase was analyzed.
- Relationships were given between conversion ratio of S, N with RH and O₃.
- Evolution of aerosol composition and particle size were analyzed.

A R T I C L E I N F O

Article history:

Received 30 June 2015

Received in revised form

23 September 2015

Accepted 25 September 2015

Available online 30 September 2015

Keywords:

Beijing hazes

Heterogeneous aqueous reactions

Inorganic aerosol

Particles size

A B S T R A C T

The effect of heterogeneous aqueous reactions on the secondary formation of inorganic aerosols during haze events was investigated by analysis of comprehensive measurements of aerosol composition and concentrations [e.g., particulate matters (PM_{2.5}), nitrate (NO₃), sulfate (SO₄), ammonium (NH₄)], gas-phase precursors [e.g., nitrogen oxides (NO_x), sulfur dioxide (SO₂), and ozone (O₃)], and relevant meteorological parameters [e.g., visibility and relative humidity (RH)]. The measurements were conducted in Beijing, China from Sep. 07, 2012 to Jan. 16, 2013. The results show that the conversion ratios of N from NO_x to nitrate (N_{ratio}) and S from SO₂ to sulfate (S_{ratio}) both significantly increased in haze events, suggesting enhanced conversions from NO_x and SO₂ to their corresponding particle phases in the late haze period. Further analysis shows that N_{ratio} and S_{ratio} increased with increasing RH, with N_{ratio} and S_{ratio} being only 0.04 and 0.03, respectively, when RH < 40%, and increasing up to 0.16 and 0.12 when RH reached 60–80%, respectively. The enhanced conversion ratios of N and S in the late haze period is likely due to heterogeneous aqueous reactions, because solar radiation and thus the photochemical capacity are reduced by the increases in aerosols and RH. This point was further affirmed by the relationships of N_{ratio} and S_{ratio} to O₃: the conversion ratios increase with decreasing O₃ concentration when O₃ concentration is lower than <15 ppb but increased with increasing O₃ when O₃ concentration is higher than 15 ppb. The results suggest that heterogeneous aqueous reactions likely changed aerosols and their precursors during the haze events: in the beginning of haze events, the precursor gases accumulated quickly due to high emission and low reaction rate; the occurrence of heterogeneous aqueous reactions in the late haze period, together with the accumulated high concentrations of precursor gases such as SO₂ and NO_x, accelerated the formation of secondary inorganic aerosols, and led to rapid increase of the PM_{2.5} concentration.

© 2015 Elsevier Ltd. All rights reserved.

* Corresponding author. Beijing Key Laboratory of Cloud, Precipitation and Atmospheric Water Resources, Beijing, China.

** Corresponding author. Beijing Key Laboratory of Cloud, Precipitation and Atmospheric Water Resources, Beijing, China.

E-mail addresses: quanjn1975@gmail.com (J. Quan), liuquan@bjmb.gov.cn (Q. Liu).

1. Introduction

Beijing has been experiencing frequent occurrence of haze events in the past two decades (Che et al., 2007; Quan et al., 2011). This severe environment problem has dire impacts on human

health, traffic, weather and climate, and other important aspects and receives growing concern in the scientific community (Charlson et al., 1987; Ramanathan and Vogelmann, 1997; Tegen et al., 2000; Yu et al., 2002; Tie et al., 2009a,b). In efforts to understand the mechanism of heavy haze formation and evolution in Beijing, many haze-related aspects have been investigated, including aerosol composition (Sun et al., 2013a,b; 2014; Huang et al., 2014), particulate matter (PM) formation mechanisms (Guo et al., 2014), regional transport of pollutants (Zhao et al., 2013a,b), hygroscopic property of particles (Pan et al., 2009; Liu et al., 2011), effects of meteorology (Zhang et al., 2015), and even the feedback between aerosols and meteorological variables (Quan et al., 2013; Gao et al., 2015). Large emission of primary aerosols and the gaseous precursors of secondary aerosols, and stagnant meteorological conditions have been usually thought as the dominant factors driving the formation and evolution of haze pollution in North China Plain (NCP, Wang et al., 2014; Guo et al., 2014; Zhang et al., 2015).

It has been reported that PM_{2.5} (particulate matter of 2.5 μm or less in aerodynamic diameter) concentration could reach as high as 600 μg m⁻³ in heavy haze events (Quan et al., 2014; Sun et al., 2014; Wang et al., 2014), and could increase by an order of magnitude in a period of 2–4 days (Quan et al., 2014; Guo et al., 2014). Meteorological conditions often play an important role in haze formation. For example, the decreased height of planetary boundary layer (PBL) in haze events suppresses particles into a shallower layer, and the weak wind slow down the horizontal transport. In addition to the meteorology factors, secondary particle formation can make a significant contribution to heavy haze events as well (Huang et al., 2014; Guo et al., 2014). Quan et al. (2014) revealed that the conversion from NO_x and SO₂ to nitrate (NO₃) and sulfate (SO₄) were likely accelerated in the late haze period. Because visibility and thus photochemical activity are low and relative humidity (RH) increases sharply in the heavy haze period, the accelerated conversion of NO_x and SO₂ might be caused by heterogeneous aqueous reactions. However, up to now the effect of heterogeneous aqueous reactions on secondary particle formation, especially in haze events, remains poorly understood and quantified.

The primary objective of this work is to investigate the effect of heterogeneous aqueous reactions on the secondary formation of inorganic aerosols during haze events based on comprehensive measurements collected during a field campaign from Sep. 7, 2012 to Jan. 16, 2013. The rest of the paper is organized as follows. Section 2 describes the instruments and measurements used in this study. The results and analysis are given in Section 3. The analysis focuses on (1) the variation of key variables in haze events, including visibility, PM_{2.5}, NO_x, SO₂, NO₃, SO₄, and the conversion ratios of N (N_{ratio}) and S (S_{ratio}); (2) the relationship of N_{ratio} and S_{ratio} with RH and O₃; (3) the evolution of mean particle diameter (D_{mean}) of submicron aerosols; and (4) contribution of heterogeneous aqueous reactions. Section 4 provides the concluding remarks.

2. Instruments and measurements

Comprehensive measurements were conducted in a field campaign at the Baolian (BL) meteorological station, China Meteorological Administration (CMA) (39°56'N, 116°17'E). The BL station located between the west 3rd and 4th highways in Beijing. The distance of the station from nearby major roads is about 400 m. The surrounding region of this site is mainly residential district, without large point sources of PM_{2.5}. A number of quantities, including atmospheric visibility, mass concentration of PM_{2.5}, chemical composition of non-refractory submicron particles (NR-PM₁), and gaseous pollutants (SO₂, NO_x, CO, O₃) were measured simultaneously, together with key meteorological variables of

temperature, RH, pressure, wind speed, and wind direction.

Detailed description of above instruments was given by Quan et al. (2013, 2014). Briefly, the mass concentration of PM_{2.5} was measured with a R&P model 1400a Tapered Element Oscillating Microbalance (TEOM, Thermo Scientific Co., USA) instrument, with a 2.5 μm cyclone inlet and an inlet humidity control system. The aerosol size distribution for particles of 13–736 nm was obtained with a Scanning Mobility Particle Sizer (SMPS, Model 3936, TSI, USA) with a time resolution of 5 min. The collocated gaseous species, including CO, SO₂, NO_x and O₃, were measured with various gas analyzers (Thermo Scientific Co., USA).

The chemical composition of NR-PM₁ was measured with an Aerodyne high-resolution Time-of-Flight Aerosol Mass Spectrometer (HRToF-AMS). The sampling time resolution was 5 min. The measured composition of particles included sulfate (SO₄), nitrate (NO₃), ammonium (NH₄), chloride (Cl), organic aerosols (ORG). The instrument was calibrated for ionization efficiency (IE) and particle sizing at the beginning, middle and end of the campaign following the standard protocols (Jimenez et al., 2003). The detection limits (DLs) of each NR-PM₁ species were determined as 3 times the standard deviations (3σ) of the corresponding signals in particle-free ambient air through a HEPA filter. As a result, the 5 min DLs of organics, sulfate, nitrate, ammonium, and chloride were 0.058, 0.006, 0.008, 0.06 and 0.016 μg m⁻³, respectively. The AMS data were analyzed for the mass concentrations and composition with the standard ToF-AMS data analysis software package (SQUIRREL version 1.50 and PIKA version 1.09) (Jimenez et al., 2003; DeCarlo et al., 2006). A collection efficiency (CE) factor of 0.5 was introduced to account for the particle loss, mostly due to particle bounce at the vaporizer (Canagaratna et al., 2007; Aiken et al., 2009; Huang et al., 2010). The values of relative ionization efficiency (RIE) used in this study were 1.2 for sulfate, 1.1 for nitrate, 1.3 for chloride and 1.4 for organics (Jimenez et al., 2003; Canagaratna et al., 2007). The RIE value of 4.0 was used for ammonium based on the analysis of pure NH₄NO₃ particles. Atmospheric visibility was measured with a PWD20 (Vaisala Co., Finland), and meteorology variables were observed by WXT-510 (Vaisala Co., Finland).

3. Results and discussion

3.1. General characteristics of haze events

The field campaign was carried out from Sep. 07, 2012 to Jan. 16, 2013, covering typical fall (Sep. 07 to Oct. 31) and winter (Nov. 01 to Jan. 16) conditions in Beijing. According to the definition by CMA that a haze event satisfies when the conditions of visibility ≤10 km and RH < 90%, there were a total of 28 haze events, with an averaged length of 4.7 days per haze event, during the experiment period (from Sep. 07, 2012 to Jan. 16, 2013). The visibility exhibits a clear periodic cycle of 4–7 days, being higher than 10 km (clean) in the beginning of each cycle, and reached around 2 km (polluted) within 2–4 days (Fig. 1a). The measured PM_{2.5} mass concentration (Fig. 1b) exhibited a similar cycle, increasing from <50 μg m⁻³ in the beginning of haze events to several hundred micrograms per cubic meter at the late stage of haze events. The NO_x (Fig. 1e) and SO₂ (Fig. 1f), as the precursors of NO₃ and SO₄, showed a cycle similar to that of PM_{2.5} concentration, with the concentrations increasing from <10 ppb in the beginning of haze events to 50–100 ppb at the late stage of haze events.

Previous studies indicated that the decreased atmospheric dispersion capacity in haze events, characterized by lowered PBL heights and weakened wind speed (Quan et al., 2013, 2014; Zhang et al., 2015), could enhance PM_{2.5} and gas pollutants concentrations. Besides that, the conversion of gas phases of N and S to

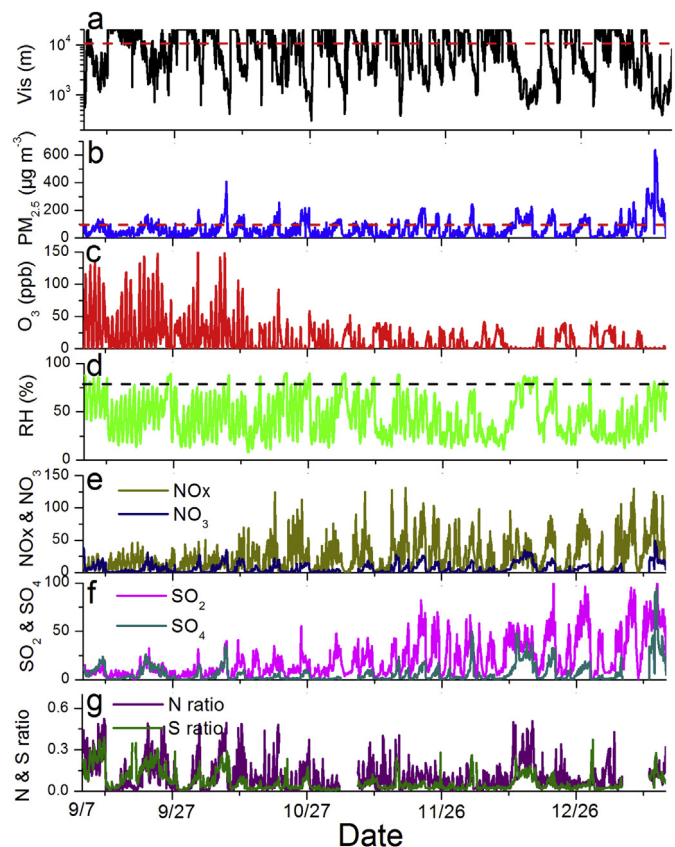


Fig. 1. Time series of visibility (a), $PM_{2.5}$ (b), O_3 (c), RH (d), NO_x (Dark yellow, ppb) and NO_3 (Navy, $\mu g m^{-3}$) (e), SO_2 (Magenta, ppb) and SO_4 (Dark cyan, $\mu g m^{-3}$) (f), and N (Purple) & S (Olive) conversion ratio (g), with time resolution of 1 h. (For interpretation of the references to color in this figure legend, the reader is referred to the web version of this article.)

particle phase as measured by the conversion ratios also increased in the haze events (Fig. 1g). The conversion ratios are defined as the ratios of the particle phase of nitrogen and sulfur to the total nitrogen and sulfur (both gas and particle phases):

$$N_{ratio} = N_a / (N_a + N_g) \quad (1)$$

$$S_{ratio} = S_a / (S_a + S_g) \quad (2)$$

where (N_{ratio}) and (S_{ratio}) denote the conversion ratios of N and S, respectively; N_a is the mass concentration of nitrogen in nitrate observed by HRTof-AMS; N_g is the mass concentration of nitrogen in NO_x , S_a is mass concentration of sulfur in sulfate observed by HRTof-AMS, and S_g is mass concentration of sulfur in SO_2 . Note that N_a and S_a were measured with AMS, which only measures nitrate and sulfate in PM_1 rather than $PM_{2.5}$. The values of N_{ratio} and S_{ratio} increased from <0.05 in the beginning of haze events to 0.2 at the end of haze events. The accelerated formation of secondary particles also helps to drive up $PM_{2.5}$ concentration in the haze events.

To get more insight into the development of haze events, the variables were classified into 4 categories based on the ranges of visibility: (a) visibility > 10 km (V1) which presents the non-haze days following the definition of CMA; (b) $10 \text{ km} \geq \text{visibility} > 5$ km (V2) for light haze days; (c) $5 \text{ km} \geq \text{visibility} > 2$ km (V3) for modest-heavy haze days; and (d) $2 \text{ km} \geq \text{visibility}$ (V4) for extreme haze days. In late haze period (V4), SO_2 concentration increased from 32.9 (V3) to 40.6 ppb (V4),

Table 1

Media values of measured visibility, particles, meteorological parameters, chemical concentrations, and S, N ratios under different visibility ranges (V1, V2, V3, and V4).

Variables	V1	V2	V3	V4
Visibility (km)	17.7	7.2	3.4	1.3
RH (%)	34.1	45.2	54.2	70.9
$PM_{2.5}$ ($\mu g m^{-3}$)	21.7	54.0	93.2	175.1
PM_1 ($\mu g m^{-3}$)	8.8	32.6	57.6	97.4
NO_x (ppb)	11.5	28.6	36.7	43.1
SO_2 (ppb)	9.1	23.5	32.9	40.6
CO (ppm)	0.6	1.6	2.4	3.7
O_3 (ppb)	19.9	14.3	15.0	4.0
N_{ratio}	0.06	0.10	0.15	0.18
S_{ratio}	0.04	0.07	0.09	0.13

enhanced by 23%, and NO_x concentration enhanced by 18% (Table 1). While for SO_4 and NO_3 , their concentration enhanced by 150% and 75%, which were much higher than that of NO_x and SO_2 . For $PM_{2.5}$, its concentration increased from 93.2 (V3) to 175.1 $\mu g m^{-3}$ (V4), enhanced by 88%. Above results indicate clearly that the conversions of gas phase of S and N to particle phase were accelerated in the late haze events. To further verify this point, the aerosol composition under different visibility conditions was studied. Fig. 2 shows the percentage of different aerosol species under the different visibility conditions. The mass concentrations of different aerosol species increased with the development of haze events from V1 to V4. In addition, the percentages of secondary aerosol particles (NO_3 , SO_4 , and NH_4) also increased. For example, in the beginning of haze events (V1), the averaged aerosol concentration is low (8.8 $\mu g m^{-3}$). The percentage of ORG is the highest (57.3%), following by SO_4 (15.7%), NO_3 (14.6%), NH_4 (9%), and Chl (3.4%). In the late period of haze events (V4), the averaged aerosol concentration reached to its highest value of 97.4 $\mu g m^{-3}$; the percentage of ORG decreased to 36.5%; the percentages of SO_4 increased to 24%; NO_3 increased to 19.4%; and NH_4 increased to 15.5%. Above analysis further confirms that the secondary formation of inorganic aerosols (e.g. nitrate and sulfate) was enhanced in the late period of haze events.

3.2. Conversion from gas to particles phases

To understand the role of heterogeneous aqueous reactions in the formation of secondary inorganic aerosols (e.g. NO_3 and SO_4), the relationships of N_{ratio} and S_{ratio} with RH were analyzed. Fig. 3 shows that N_{ratio} and S_{ratio} have no significant variation when $RH < 40\%$. After $RH > 40\%$, both N_{ratio} and S_{ratio} increased with further increase of RH. For example, N_{ratio} and S_{ratio} were only 0.03 and 0.03 when RH was lower than 40%, and increased to 0.20 and 0.15 when RH reached 60–80% (Fig. 3a and b). Some aerosol particles likely experience hygroscopic growth under high RH, depending mainly on size, composition and RH. For example, the theoretical deliquescence point of NaCl is about 75%, and mixing of organics could decrease the deliquescence point (Hansson et al., 1998). The field experiment indicates that particles begin hygroscopic growth around 40% (Pan et al., 2009). After that, the hygroscopic growth factor increased exponentially. The aerosol composition in Beijing contained a large amount of hydrophilic aerosol particles, such as ammonium sulfate and ammonium nitrate (Sun et al., 2013a). These hydrophilic aerosol particles have a strong hygroscopic property, and their radii can be doubled, or approximate 8 times increase of particle volume, under high RH value (Liu et al., 2011), which provides an excellent substrate for heterogeneous aqueous reactions. The increase of N_{ratio} and S_{ratio} with RH (Fig. 3) suggests that heterogeneous aqueous reactions play important role in the secondary formation of inorganic aerosols in haze events. High

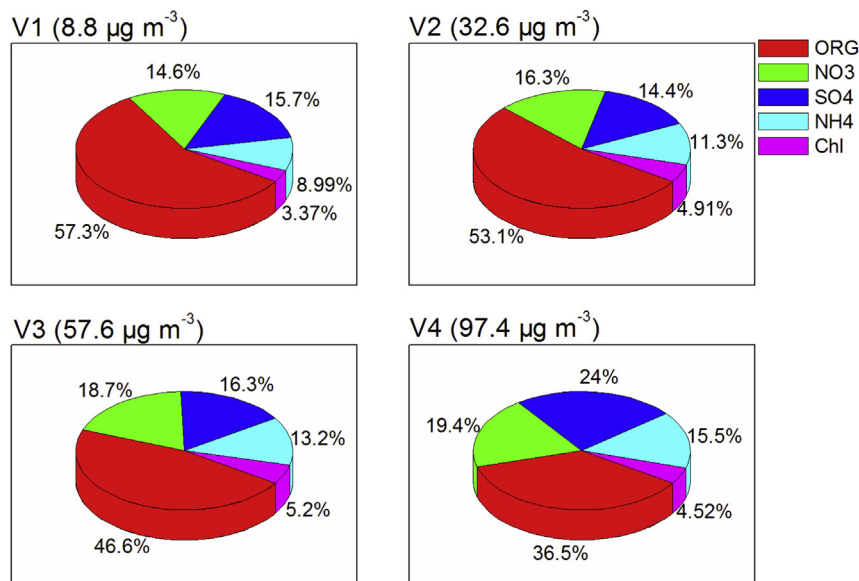


Fig. 2. Aerosol composition measured by AMS under different visibility conditions. The 4 conditions are classified as: visibility >10 km (V1), 10 km \geq visibility > 5 km (V2), 5 km \geq visibility > 2 km (V3), and 2 km \geq visibility (V4).

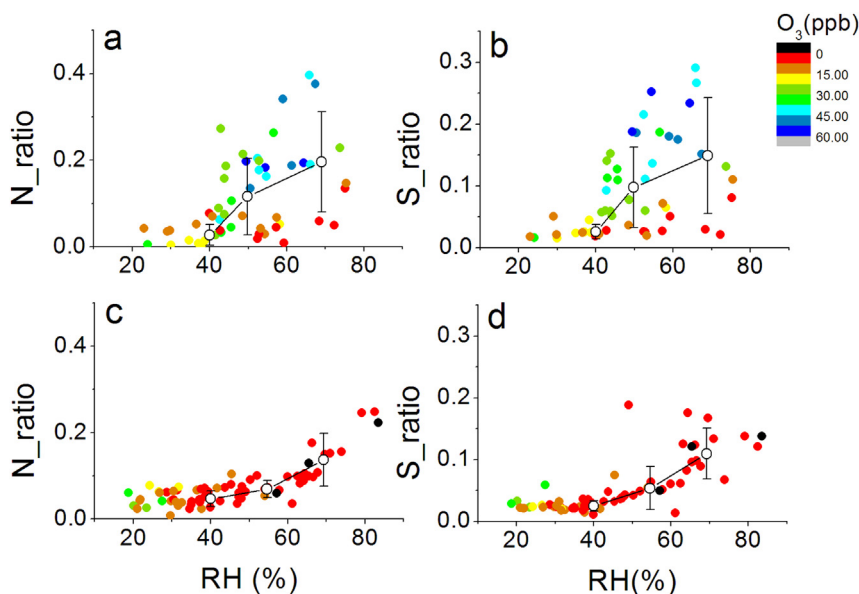


Fig. 3. Relationship between N_{ratio} , S_{ratio} and RH in fall (a, b) and winter (c, d), with time resolution of 1 day. The dot line is averaged value, with standard deviation, under RH of <40%, 40–60%, 60–80%.

photochemical activity, represented by a high O_3 concentration, would further enhance the conversion ratios (Fig. 3).

In order to further understand the mechanisms of the formation of NO_3 and SO_4 in haze events, especially the relative role of photochemical and heterogeneous aqueous activities, the relationships of conversion ratios of N and S with O_3 were analyzed. Fig. 4 shows that N_{ratio} and S_{ratio} were the lowest when the daily-averaged O_3 concentration was 15–20 ppb. Above this range, the ratios increased with O_3 . For example, N_{ratio} and S_{ratio} were 0.04 and 0.03 when O_3 ranging 15–20 ppb, and increased to 0.23 and 0.20 when O_3 ranging 40–60 ppb. These results reflect the role of photochemical activity in the formation of NO_3 and SO_4 , indicating that higher photochemical capacity will enhance the conversion of gas phases of N and S to particle phases. Another interesting aspect

shown in Fig. 4 was that the conversion ratios of N and S also increased with decrease of O_3 concentration when the daily-averaged O_3 concentration was lower than 15 ppb. For example, the transfer ratios of N and S increased to 0.10 and 0.07 when O_3 was lower than 2 ppb. The opposite changes of O_3 and RH (O_3 decreased while RH increased) reinforce the notion that the increased conversion ratios of N and S was caused dominantly by heterogeneous aqueous reactions.

The O_3 concentration in winter was lower than in autumn (Fig. 1c), indicating that photochemical capacity in winter was lower than in autumn and the relative role of photochemical and heterogeneous aqueous activities in the secondary formation of inorganic aerosols might be different between the two seasons. The conversion ratios of N and S were higher in autumn than in winter

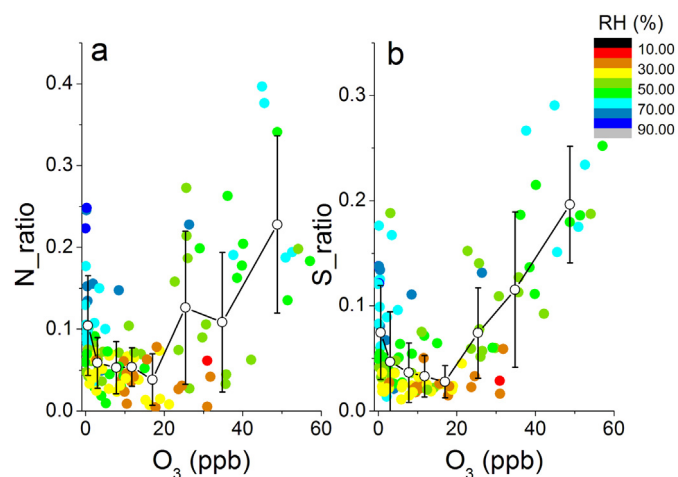


Fig. 4. Relationship between N_{ratio} (a), S_{ratio} (b) and O_3 , with time resolution of 1 day. The dot line is averaged value, with standard deviation, under O_3 of <2, 2–5, 5–10, 10–15, 15–20, 20–30, 30–40, 40–60 ppb.

under same RH conditions (Fig. 3). For example, N_{ratio} and S_{ratio} increased from 0.03 to 0.20, and 0.03 to 0.15 when RH increased from <40% to 60–80% in autumn. In this process, the O_3 concentration also increased from 14.6 to 26.4 ppb. While in winter, N_{ratio} and S_{ratio} only increased to 0.14 and 0.11, but the O_3 concentration decreased from 9.9 to 2.5 ppb. These results indicate that the high conversion of S and N in haze events was caused by the combined effect of photochemical and heterogeneous aqueous activity in autumn. While in winter, the contribution of the heterogeneous aqueous activity became more important to the formation of the secondary inorganic aerosols in haze events.

3.3. Evolution of particle size in haze events

To further understand the role of heterogeneous aqueous reactions in haze events, evolution of particle size was analyzed. The mean particle diameter (D_{mean}) is calculated as follow:

$$D_{\text{mean}} = \frac{\sum n_i D_i}{\sum n_i} \quad (3)$$

where n_i particles are observed in the i -th bin of SMPS; D_i is the arithmetic mean radius of upper and lower limitation of i -th bin. It is interesting to note that D_{mean} (Fig. 5b) shows a cycle similar to that of the mass concentration (Fig. 5a). With the development of haze events, the mean diameter increased from 50 nm to 150–200 nm in 2–4 days. The variation of particle number concentration (Fig. 5c) was not as discernible as that of particles size, indicating that the increased $PM_{2.5}$ concentration in haze events was caused primarily by particle growth. As we know, atmospheric particles originate from two main sources: primary emitted particles and secondary formed particles arising from new particle formation (NPF) processes. After that, it grows into relevant size range by condensation of chemical species such as sulfate, nitrate, and organic compounds that have been partially oxidized in the atmosphere. NPF events usually occur in clean condition, because high concentration of preexisting particles will suppress aerosol nucleation and NPF in heavy pollution (Guo et al., 2014). Typically, new particle formation and growth occur on a daily cycle in most regions worldwide (Zhang et al., 2012), but few other locations exhibit particle growth as sustained (2–4 d) and efficient as those displayed during the transition and polluted periods in Beijing (Guo et al., 2014). In haze events, RH increased gradually (Fig. 1d). Under

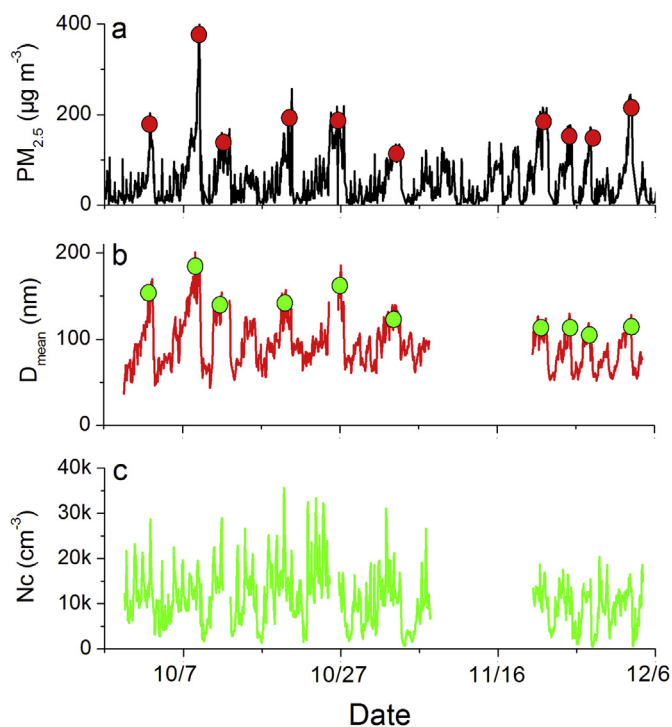


Fig. 5. Time series of $PM_{2.5}$ mass concentration (a), mean diameter (b) and number concentration (N_c , c) of submicron aerosols (13–736 nm) measured by SMPS, with time resolution of 1 h.

high RH, water vapor will be absorbed onto particle surface that can serve as good substrate for heterogeneous aqueous reactions. Hence, the increased particle size in haze event might attribute to heterogeneous aqueous reactions. We further analyze the relationship between mean diameter and RH (Fig. 6). The results indicate that particle size didn't vary much with RH when RH <40%, but increased significantly with RH when RH >40%. This result was consistent with the hygroscopic growth of aerosols under different values of RH and the relationship of conversion ratios of S and N with RH discussed earlier, and further lends support to the importance of heterogeneous aqueous reactions in haze events.

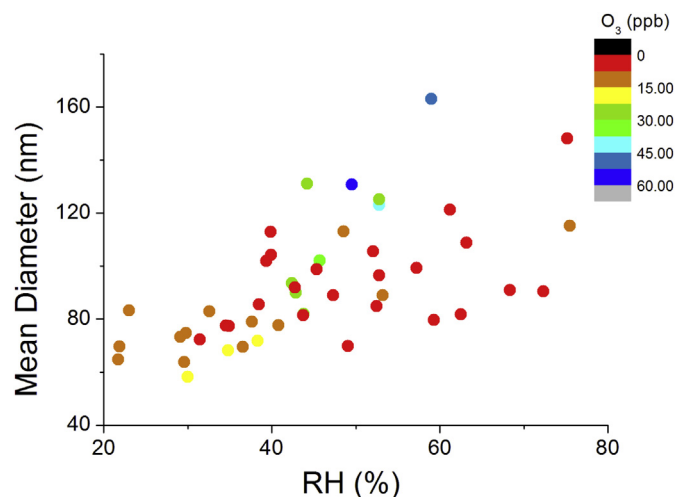


Fig. 6. Relationship between mean diameter of submicron aerosols and RH, with time resolution of 1 day.

3.4. Contributions of heterogeneous aqueous reactions in haze events

Secondary aerosol species contribute a major fraction of the total PM_{2.5} in Beijing (Huang et al., 2014). For secondary aerosols, the variation of conversion rate in process of gas to particle will affect their mass concentration directly, together with the concentration of their precursor gases. Based on our measurements, the average period of a haze event is 4.7 days. The averaged duration in the 4 stages were 2.02 days (V1), 0.90 days (V2), 1.03 days (V3), and 0.76 days (V4). In the beginning period of haze events, the concentration of SO₄ increased from 1.44 μg m⁻³ (V1) to 4.67 μg m⁻³ (V2), with increase rate of 1.60 μg m⁻³ d⁻¹. While in the late period of haze events (V4), the concentration of SO₄ increased to 23.44 μg m⁻³ (V4), with increase rate of 10.49 μg m⁻³ d⁻¹. The increase rate of SO₄ was significantly accelerated in the late stage (V4) of haze events. While for SO₂, its concentration reached 23.5 ppb in the V2 stage, with increase rate of 8.05 ppb d⁻¹, and increased to 40.5 ppb in the V4 stage, with increase rate of 9.50 ppb d⁻¹. The variation of NO_x and NO₃ also show similar trends. As the analysis in Section 3.2 and 3.3, the involvement of heterogeneous aqueous reactions might be the dominant factor that accelerated the formation of SO₄ and NO₃ in the late haze events. Supposing the increase rate of SO₄ in the late period were the same as the beginning period, the SO₄ concentration might only reach to 7.53 μg m⁻³ in the V4 stage, much lower than the actual value (23.44 μg m⁻³). Therefore, the participation of heterogeneous aqueous reactions changed the variation of aerosols and their precursors in haze events. In the beginning period of haze events, the precursor gases accumulate quickly due to high emission and low reaction rate. The involvement of heterogeneous aqueous reactions, together with the accumulated high precursor gases, e.g. SO₂ and NO_x, accelerated the formation of secondary inorganic aerosols, and led to the rapid increase of PM_{2.5} concentration in the late haze period.

4. Summary

The effect of heterogeneous aqueous reactions on the secondary formation of inorganic aerosols in haze events are investigated by analyzing the comprehensive measurements collected during a field campaign in Beijing. The major results are summarized below:

- (1) The conversion of gas phase of S and N to particle phase was accelerated in late haze events. For example, the conversion ratios, N_{ratio} and S_{ratio} , increased from 0.06 to 0.18, and 0.04 to 0.13 from the beginning to the late periods of haze events. Analysis shows that N_{ratio} or S_{ratio} with RH increased with increasing RH when RH was higher than 40%. When RH < 40%, N_{ratio} or S_{ratio} showed no significant variation with RH. The threshold RH of ~40% suggests that particles began hygroscopic growth after that. Under high RH value (80%), the radius of aerosol particles could be doubled by coating with the water vapor on the particle surface, which provides an excellent carrier for heterogeneous aqueous reactions. This point was further reinforced by the relationships of N_{ratio} and S_{ratio} with O₃ concentration. N_{ratio} and S_{ratio} were lowest when the daily-averaged O₃ ranges between 15 and 20 ppb. Above this O₃ range, N_{ratio} and S_{ratio} increased with the increase of O₃ concentration whereas N_{ratio} and S_{ratio} increased with the decrease of O₃ concentration below this O₃ range. The results suggest that the conversion of gas phase of S and N to particle phase might be affected by two different mechanisms. Besides photochemical reactions, heterogeneous aqueous reactions might also play important role in

the secondary formation of inorganic aerosols. The photochemical capacity usually decrease in the late period of haze events due to the decreased solar radiation caused by increased aerosols, so the increased conversion ratios of S and N in late haze might be caused by heterogeneous aqueous reactions since RH increased evidently in this period.

- (2) In haze events, the mean diameter of particles exhibited a cycle similar to that of the PM_{2.5} mass concentration. With the development of haze events, the mean diameter increased from 50 nm to 150–200 nm in 2–4 days. The variation of particle number concentration was not as discernible as that of particles size, indicating that the increased PM mass concentration in haze events was dominated by the enhanced particle size (growth). The relationship of mean diameter of particles with RH indicated that the mean diameter increased with the increase of RH when RH was higher than 40%, while when RH is lower than 40%, particle size did not vary much with RH. The result was consistent with the relationship of N_{ratio} and S_{ratio} to RH and with the hygroscopic growth of aerosols under different values of RH, and further reinforced the important contribution of heterogeneous aqueous reactions in haze events.
- (3) The participation of heterogeneous aqueous reactions changed the variation of aerosols and their precursors in haze events. In the beginning period of haze events, the precursor gases accumulated quickly due to high emission and low reaction rate. Heterogeneous aqueous reactions, together with the accumulated high precursor gases (e.g. SO₂ and NO_x) accelerated the formation of secondary inorganic aerosols, resulting in rapid increase of the PM_{2.5} concentration in the late haze period.

It is noteworthy that besides the conversion of SO₂/NO_x by photochemical reactions or heterogeneous aqueous reactions, sulfate/nitrate might also derive from the transportation from the layer above where photochemical reactivity was stronger as a result of light reflection by concentrated particles below it. This process may impact estimation of the role of heterogeneous aqueous reactions, and deserves in-depth study in the future.

Acknowledgments

This research is partially supported by Projects of Beijing Municipal Science & Technology Commission under Grant No. Z141100001014017, No. 8144049. This research is also partially supported by the National Basic Research Program of China (2011CB403401) and the National Natural Science Foundation of China (41405127). Y. Liu is supported by the US Department of Energy's Atmospheric System Research (ASR) program.

References

- Aiken, A.C., Salcedo, D., Cubison, M.J., Huffman, J.A., DeCarlo, P.F., Ulbrich, I.M., Docherty, K.S., Sueper, D., Kimmel, J.R., Worsnop, D.R., Trimborn, A., Northway, M., Stone, E.A., Schauer, J.J., Volkamer, R.M., Fortner, E., de Foy, B., Wang, J., Laskin, A., Shutthanandan, V., Zheng, J., Zhang, R., Gaffney, J., Marley, N.A., Paredes-Miranda, G., Arnott, W.P., Molina, L.T., Sosa, G., Jimenez, J.L., 2009. Mexico City aerosol analysis during MILAGRO using high resolution aerosol mass spectrometry at the urban supersite (T0) – Part 1: Fine particle composition and organic source apportionment. *Atmos. Chem. Phys.* 9 (17), 6633–6653.
- Canagaratna, M.R., Jayne, J.T., Jimenez, J.L., Allan, J.D., Alfarra, M.R., Zhang, Q., Onasch, T.B., Drewnick, F., Coe, H., Middlebrook, A., Delia, A., Williams, L.R., Trimborn, A.M., Northway, M.J., DeCarlo, P.F., Kolb, C.E., Davidovits, P., Worsnop, D.R., 2007. Chemical and microphysical characterization of ambient aerosols with the aerodyne aerosol mass spectrometer. *Mass Spectrom. Rev.* 26 (2), 185–222.

- Charlson, R.J., Lovelock, J.E., Andreae, M.O., Warren, S.G., 1987. Oceanic phytoplankton, atmospheric sulfur, cloud albedo and climate. *Nature* 326, 655–661.
- Che, H., Zhang, X., Li, Y., Zhou, Z., Qu, J.J., 2007. Horizontal visibility trends in China 1981–2005. *Geophys. Res. Lett.* 34, L24706.
- DeCarlo, P.F., Kimmel, J.R., Trimborn, A., Northway, M.J., Jayne, J.T., Aiken, A.C., Gonin, M., Fuhrer, K., Horvath, T., Docherty, K.S., Worsnop, D.R., Jimenez, J.L., 2006. Field-deployable, high-resolution, time-of-flight aerosol mass spectrometer. *Anal. Chem.* 78 (24), 8281–8289.
- Gao, Y., Zhang, M., Liu, Z., Wang, L., Wang, P., Xia, X., Tao, M., Zhu, L., 2015. Modeling the feedback between aerosol and meteorological variables in the atmospheric boundary layer during a severe fog–haze event over the North China Plain. *Atmos. Chem. Phys.* 15, 4279–4295.
- Guo, S., Hu, M., Zamora, M.L., Peng, J.F., Shang, D.J., Zheng, J., Du, Z., Wu, Z., Shao, M., Zeng, L., Molina, M.J., Zhang, R., 2014. Elucidating severe urban haze formation in China. *Proc. Natl. Acad. Sci.* 111, 17373–17378.
- Hansson, H.C., Rood, M.J., Koloutsou-Vakakis, S., Hameri, K., Orsini, D., Wiedensohler, A., 1998. NaCl aerosol particle hygroscopicity dependence on mixing with organic compounds. *J. Atmos. Chem.* 31, 321–346.
- Huang, R.J., Zhang, Y., Bozzetti, C., Ho, K.F., Cao, J.J., Han, Y., Daellenbach, K.R., Slowik, J.G., Platt, S.M., Canonaco, F., Zotter, P., Wolf, R., Pieber, S.M., Bruns, E.A., Crippa, M., Ciarelli, G., Piazzalunga, A., Schwikowski, M., Abbaszade, G., Schnelle-Kreis, J., Zimmermann, R., An, Z., Szidat, S., Baltensperger, U., El Haddad, I., Prévôt, A.S., 2014. High secondary aerosol contribution to particulate pollution during haze events in China. *Nature* 514, 218–222.
- Huang, X.F., He, L.Y., Hu, M., Canagaratna, M.R., Sun, Y., Zhang, Q., Zhu, T., Xue, L., Zeng, L.W., Liu, X.G., Zhang, Y.H., Jayne, J.T., Ng, N.L., Worsnop, D.R., 2010. Highly time-resolved chemical characterization of atmospheric submicron particles during 2008 Beijing Olympic Games using an aerodyne high-resolution aerosol mass spectrometer. *Atmos. Chem. Phys.* 10, 8933–8945.
- Jimenez, J.L., Jayne, J.T., Shi, Q., Kolb, C.E., Worsnop, D.R., Yourshaw, I., Seinfeld, J.H., Flagan, R.C., Zhang, X., Smith, K.A., Morris, J.W., Davidovits, P., 2003. Ambient aerosol sampling using the aerodyne aerosol mass spectrometer. *J. Geophys. Res.* 108, 8425.
- Liu, P.F., Zhao, C.S., Gobel, T., Hallbauer, E., Nowak, A., Ran, L., Xu, W.Y., Deng, Z.Z., Ma, N., Mildenberger, K., Henning, S., Stratmann, F., Wiedensohler, A., 2011. Hygroscopic properties of aerosol particles at high relative humidity and their diurnal variations in the North China Plain. *Atmos. Chem. Phys.* 11, 3479–3494.
- Pan, X.L., Yan, P., Tang, J., Ma, J.Z., Wang, Z.F., Gbaguidi, A., Sun, Y.L., 2009. Observational study of influence of aerosol hygroscopic growth on scattering coefficient over rural area near Beijing mega-city. *Atmos. Chem. Phys.* 9, 7519–7530.
- Quan, J.N., Zhang, Q., Liu, J.Z., Huang, M.Y., Jin, H., 2011. Analysis of the formation of fog and haze in North China Plain (NCP). *Atmos. Chem. Phys.* 11, 8205–8214.
- Quan, J.N., Gao, Y., Zhang, Q., Tie, X.X., Cao, J., Han, S., Meng, J., Chen, P., Zhao, D., 2013. Evolution of planetary boundary layer under different weather conditions, and its impact on aerosol concentrations. *Particology* 11, 34–40.
- Quan, J.N., Tie, X., Zhang, Q., Liu, Q., Li, X., Gao, Y., Zhao, D., 2014. Characteristics of heavy aerosol pollution during the 2012–2013 winter in Beijing, China. *Atmos. Environ.* 88, 83–89.
- Ramanathan, V., Vogelmann, A.M., 1997. Greenhouse effect, atmospheric solar absorption, and the earth's radiation budget: from the Arrhenius–Lanely era to the 1990s. *Ambio* 26 (1), 38–46.
- Sun, Y.L., Wang, Z.F., Fu, P.Q., Yang, T., Jiang, Q., Dong, H.B., Li, J., Jia, J.J., 2013a. Aerosol composition, sources and processes during wintertime in Beijing, China. *Atmos. Chem. Phys.* 13, 4577–4592.
- Sun, Y.L., Wang, Z., Fu, P., Jiang, Q., Yang, T., Li, J., Ge, X., 2013b. The impact of relative humidity on aerosol composition and evolution processes during wintertime in Beijing, China. *Atmos. Environ.* 77, 927–934.
- Sun, Y., Jiang, Q., Wang, Z., Fu, P., Li, J., Yang, T., Yin, Y., 2014. Investigation of the sources and evolution processes of severe haze pollution in Beijing in January 2013. *J. Geophys. Res.* 114, 4380–4398.
- Tegen, I., Koch, D., Lacis, A.A., Sato, M., 2000. Trends in tropospheric aerosol loads and corresponding impact on direct radiative forcing between 1950 and 1990: a model study. *J. Geophys. Res.* 105, 26971–26990.
- Tie, X., Madronich, S., Li, G.H., Ying, Z.M., Weinheimer, A., Apel, E., et al., 2009a. Simulation of Mexico City plumes during the MIRAGE-Mex field campaign using the WRF-Chem model. *Atmos. Chem. Phys.* 9, 4621–4638.
- Tie, X., Wu, D., Brasseur, G., 2009b. Lung cancer mortality and exposure to atmospheric aerosol particles in Guangzhou, China. *Atmos. Environ.* 43, 2375–2377.
- Wang, Y.S., Yao, L., Wang, L.L., Liu, Z., Ji, D., Tang, G., Zhang, J., Sun, Y., Hu, B., Xin, J., 2014. Mechanism for the formation of the January 2013 heavy haze pollution episode over central and eastern China. *Sci. China Earth Sci.* 57, 14–25.
- Yu, H., Liu, S.C., Dickinson, R.E., 2002. Radiative effects of aerosols on the evolution of the atmospheric boundary layer. *J. Geophys. Res.* 107, 4142. <http://dx.doi.org/10.1029/2001JD000754>.
- Zhang, Q., Quan, J.N., Tie, X., Li, X., Liu, Q., Gao, Y., Zhao, D., 2015. Effects of meteorology and secondary particle formation on visibility during heavy haze events in Beijing, China. *Sci. Total Environ.* 502, 578–584.
- Zhang, R., Khalizov, A., Wang, L., Hu, M., Xu, W., 2012. Nucleation and growth of nanoparticles in the atmosphere. *Chem. Rev.* 112 (3), 1957–2011.
- Zhao, P.S., Dong, F., He, D., Zhao, X.J., Zhang, X.L., Zhang, W.Z., Yao, Q., Liu, H.Y., 2013a. Characteristics of concentrations and chemical compositions for PM_{2.5} in the region of Beijing, Tianjin, and Hebei, China. *Atmos. Chem. Phys.* 13, 4631–4644.
- Zhao, X.J., Zhao, P.S., Xu, J., Meng, W., Pu, W.W., Dong, F., He, D., Shi, Q.F., 2013b. Analysis of a winter regional haze event and its formation mechanism in the North China Plain. *Atmos. Chem. Phys.* 13, 5685–5696.